Chorus functional dependencies derived from CRRES data

M. Spasojevic[1] and Y. Y. Shprits[2,3,4]

Received 20 June 2013; revised 11 July 2013; accepted 12 July 2013.

[1] Using data from the Combined Release and Radiation Effects Satellite (CRRES) plasma wave experiment, we present quadratic fits to the mean of the wave amplitude squared, $< B_w^2 >$, for lower and upper band chorus as a function of geomagnetic activity (Kp) and magnetic latitude (λ) for the midnight ($21<MLT\leq3$), dawn ($3<MLT\leq9$), and postnoon ($12<MLT\leq15$) sectors and present an ad hoc model for the prenoon ($9<MLT\leq12$) sector. The empirical models are valid for $4\leq L \leq7$, $|\lambda| < 15°$ and $Kp\leq6$ and quantify the dramatic difference in the latitudinal dependence of chorus as a function of local time and how that dependence varies with geomagnetic condition, critical parameters for calculating wave-induced electron scattering rates. Our results are generally consistent with previous studies, and our key contribution is the quantification of wave properties in a manner that is easily incorporated into global quasi-linear diffusion models. **Citation:** Spasojevic, M., and Y. Y. Shprits (2013), Chorus functional dependencies derived from CRRES data, *Geophys. Res. Lett.*, *40*, doi:10.1002/grl.50755.

1. Introduction

[2] Intense whistler-mode chorus emissions permeate the Earth's magnetosphere, and there is considerable evidence that these waves are a significant driver of both energetic electron acceleration and loss (see reviews by *Shprits et al.* [2008a], *Shprits et al.* [2008a], *Shprits et al.* [2008b]; *Millan and Baker* [2012], and *Millan and Baker* [2012]). The effects of chorus have been included in quasi-linear diffusion models with results indicating the chorus plays a major and possibly dominant role in the formation of the outer belt [e.g., *Thorne*, 2010]. Accurate modeling of electron dynamics in diffusion analysis requires empirical models of chorus properties including wave amplitude, spectral distribution, and wave normal angle as function of L, magnetic local time (MLT), magnetic latitude (λ), and geomagnetic conditions. In particular, in the approximation of the quasi-linear theory, pitch angle, energy, and mixed scattering rates are proportional to the square of the wave amplitude. The amplitude of chorus waves may vary by two orders of magnitude, resulting in four orders of magnitude in scattering rates and consequently four orders of magnitude change in acceleration and loss rates. Thus, accurate wave parametrizations are critical to modeling radiation belt dynamics.

[3] Several spacecraft missions have provided data for chorus analysis [e.g., *Agapitov et al.*, 2012; *Bunch et al.*, 2012; *Golden et al.*, 2012; *Meredith et al.*, 2012], but the Combined Release and Radiation Effects Satellite (CRRES) mission from 1990–1991 provided the statistics mostly widely used in global diffusion calculations as a result of the favorable spatial coverage in the heart of the outer belt acceleration region during a period of solar maximum. CRRES provides good coverage of the near-equatorial region, which is not well sampled by spacecraft with polar or highly elliptical orbits. *Meredith et al.* [2003a] presented plots of chorus wave intensity for low ($< 15°$) and high ($> 15°$) magnetic latitude as a function of radial distance and MLT for three levels of geomagnetic activity. There have been several attempts to parametrize the CRRES wave maps for inclusion into diffusion models. *Shprits et al.* [2007] derived an analytical dependence for the wave amplitude on geomagnetic activity, but since the work focused on the loss of relativistic electrons on the dayside, parameterization was done using measurements on the dayside at high latitudes, and waves at other local times and latitudes, which play a very important role in acceleration and particle loss, were not considered. In the work of *Shprits et al.* [2006] and *Li et al.* [2007], chorus parameterizations with latitude were taken from the visual inspection of the figures of previously published results. In further work, the derived dayside dependence on geomagnetic activity from high latitudes was adopted to all MLT and latitudes [e.g., *Subbotin et al.*, 2011; *Kim et al.*, 2012]. While these ad hoc parametrizations have been sufficient to infer general trends of acceleration and loss in the two-dimensional pitch angle and energy code, the newly developed three- and four-dimensional codes, which account for diffusion in radial distance, pitch angle, energy, and mixed diffusion, require significantly improved wave parameterizations.

[4] The goal of this study is to provide an analytical parameterization of time-averaged chorus magnetic field intensity $< B_w^2 >$ as a function of MLT, λ, L, and geomagnetic activity for easy inclusion into global 3-D and 4-D diffusion codes. Recently, *Meredith et al.* [2012] presented wave maps formed by combining data from five spacecraft missions. However, inferring analytical relationships for such combined data sets is a challenging task as satellites may not be properly intercalibrated and may have a particular bias associated with the spatial and solar cycle coverage of the satellites as well as differing instrument resolution and sensitivity. Thus, in this initial study, we focus on developing an analytical wave model using only the CRRES mission. Our larger goal is to incorporate additional data sets after performing intercalibrations within regions of spatial and geomagnetic overlap and to present to the community

Additional supporting information may be found in the online version of this article.

[1]Department of Electrical Engineering, Stanford University, Stanford, California, USA.
[2]Skolkovo Institute of Science and Technology, Moscow, Russia.
[3]Earth and Space Sciences, UCLA, Los Angeles, California, USA.
[4]Department of Earth, Atmospheric, and Planetary Sciences, MIT, Cambridge, Massachusetts, USA.

Corresponding author: M. Spasojevic, Department of Electrical Engineering, Stanford University, 350 Serra Mall, Packard Bldg. Rm. 321, Stanford, CA 94305-9515, USA. (mariaspasojevic@stanford.edu)

0094-8276/13/10.1002/grl.50755

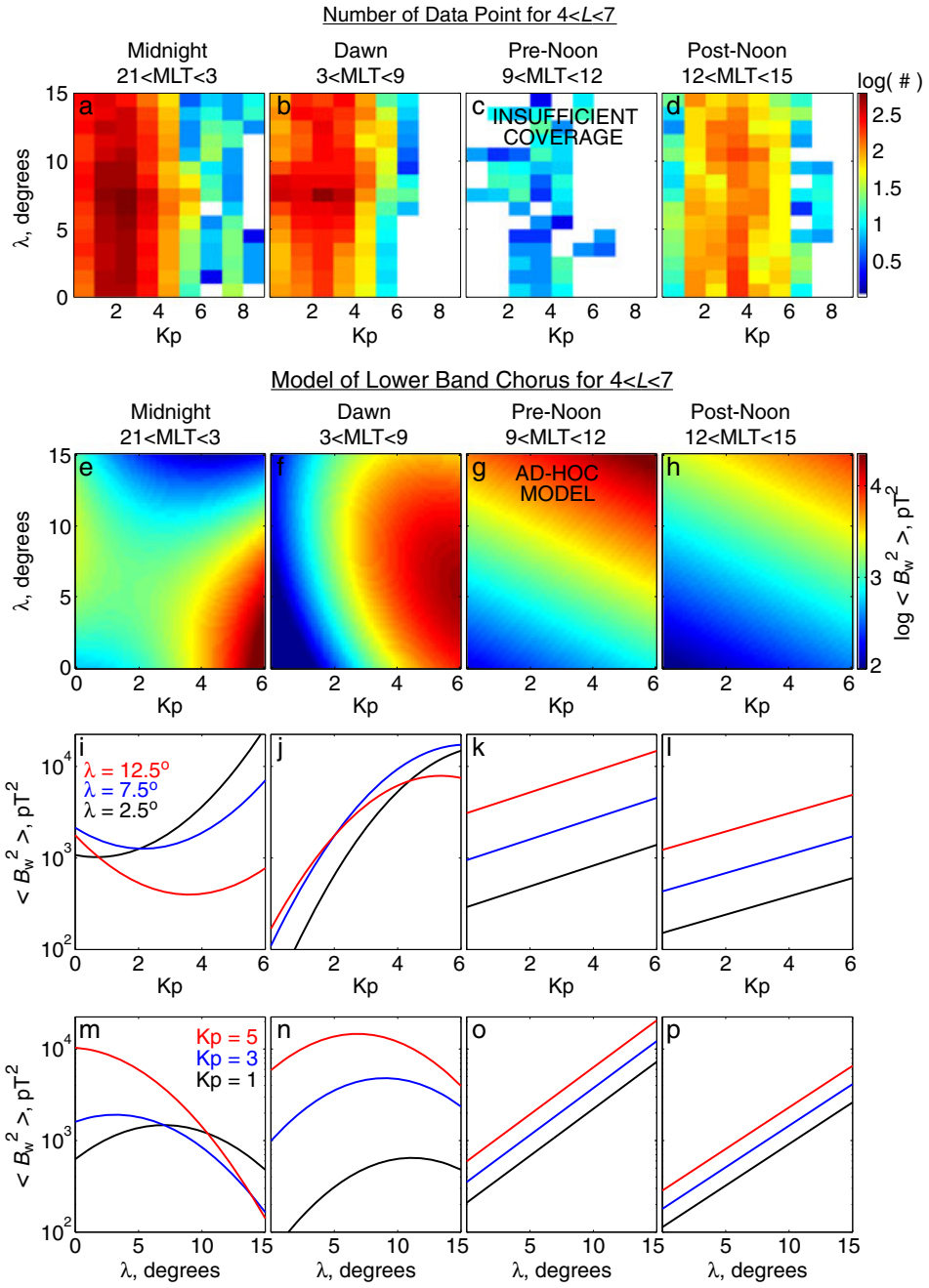

Figure 1. The number of data points available for analysis as a function of Kp and λ in the range of $4 \leq L \leq 7$ for each of four local time sectors (a, b, c, d). Two-dimensional output of the lower band chorus model (e, f, g, h). Variation with Kp at three values of λ (i, j, k, l). Variation with λ for three values of Kp (m, n, o, p).

wave parametrizations in terms of simple polynomial fits to $< B_w^2 >$.

2. Data Analysis

[5] CRRES was a U.S. Air Force mission designed to study the near-Earth radiation environment and launched in a 350 km altitude × 6.3 R_E geocentric orbit with an inclination of 18.1° [*Johnson and Kierein*, 1992]. The CRRES plasma wave experiment included a 128-step sweep frequency receiver (SFR) covering 100 Hz to 400 kHz from a single 100 m tip-to-tip electric dipole antenna oriented perpendicular to the spacecraft spin axis, which was in the ecliptic plane [*Anderson et al.*, 1992]. Analysis presented here uses a database of SFR recordings covering 19 August 1990 to 12 October 1991 (orbits 61–1067). To eliminate effects of the spacecraft spin, we use 3 min averages of the electric (E) field spectral density. Since pitch angle and energy diffusion rates scale as a function of wave magnetic (B) field, we convert the E-field spectral densities to B-field using the parallel propagating whistler-mode dispersion relationship along with measurements of the local background magnetic field (B_o) and estimates of the cold plasma density derived from the upper hybrid resonance line observed in the higher frequency bands of the SFR [*Ledocq et al.*, 1994], similar to *Meredith et al.* [2003b]. Wave amplitude is computed for all intervals when the spacecraft is outside

Table 1. Table of Weights for the Polynomial Fit Described by Equation (1) and the Resulting Coefficient of Determination, R^2

Band, Local Time	w_0	w_1	w_2	w_3	w_4	w_5	R^2
Lower, midnight	2.743	0.004073	0.1356	–0.02915	0.05010	–0.007611	0.54
Lower, dawn	0.9617	0.8528	0.2080	–0.01829	–0.05829	–0.008535	0.63
Lower, prenoon (ad hoc)	2.207	0.1131	0.1027	0	0	0	—
Lower, postnoon	1.953	0.1001	0.09089	0	0	0	0.45
Upper, midnight	0.7698	0.6764	–0.06983	–0.02759	–0.03954	0	0.76
Upper, dawn	1.669	0.5493	–0.2481	0	–0.04982	0.008420	0.66
Upper, prenoon (ad hoc)	1.247	0.5351	–0.1506	–0.01115	–0.04365	0.006748	—
Upper, postnoon	–0.2421	0.5327	0.1692	–0.01616	–0.04592	–0.007204	0.23

the plasmapause as determined by the database of CRRES plasmapause locations compiled by *Moldwin et al.* [2002]. In slight contrast to *Meredith et al.* [2012], we calculate the total wave amplitude (B_w) by integrating the B-field spectral density across the chorus band as defined by an estimate of the equatorial electron gyrofrequency (f_{ce-eq}) rather than the local gyrofrequency [e.g., *Burtis and Helliwell*, 1976]. f_{ce-eq} is estimated by using the measured B_o and assuming a dipolar scaling along field lines to the equator. Here we define lower band chorus as extending from $0.05 < f_{ce-eq} < 0.5$ and upper band chorus as extending from $0.5 < f_{ce-eq} < 0.95$. In analyzing the effect of the different normalization techniques, we find that the difference in calculated wave amplitude is more pronounced for upper band chorus. Scaling by local gyrofrequency tends to underestimate wave amplitude in the off-equatorial region since as B_o increases, the waves are shifted to lower normalized frequency, and the relatively narrowband upper band chorus emissions may be shifted below the defined band of integration.

[6] Although the CRRES spacecraft routinely made measurements up to $\sim 30°$ latitude, in this study we limit our analysis to waves within 15°. This decision was made as a result of concerns in the reliability of using the assumption of parallel propagation at the higher latitudes. Statistics on chorus wave normal angles in the off-equatorial region are relatively sparse, but work by *Haque et al.* [2010] found that in the latitude range of 10°–25°, over 50% of lower band and over 85% of upper band chorus measurements had wave normal angles greater than 30°. Assuming parallel propagation in these regions may result in a significant overestimation of B_w.

[7] Our original intention was to develop an empirical chorus model as a function of geomagnetic activity, λ, and L. However, initial analysis indicated that the dependence on L was relatively weak over the range $4 \leq L \leq 7$. Thus, to improve statistics in the other parameters, we chose to remove the L dependence. We use the Kp index to parametrize the geomagnetic variability since it most widely used input to global diffusion codes. Past work [e.g., *Bunch et al.*, 2011, 2012] found that chorus is well characterized by division into three 6 hour local time sectors centered at 0, 6, and 12 MLT. Unfortunately, CRRES had extremely poor coverage in the prenoon sector (Figure 1c). After experimentation, we have chosen to divide the data into three local time sectors, where midnight is $21<\text{MLT}\leq 3$, dawn is $3<\text{MLT}\leq 9$, and postnoon is $12<\text{MLT}\leq 15$, and an empirical model is developed separately for each sector. For the prenoon sector ($9<\text{MLT}\leq 12$), we construct an ad hoc model of chorus by combining properties of both the dawn and postnoon sectors, as described below. Figures 1a–1d show the number of data points available for analysis in the range of $4 \leq L \leq 7$ as a function of Kp and λ for each local time sector. As noted, the prenoon sector has insufficient statistics, but for the other local time sectors, coverage is good across the entire latitude range for low and moderate values of Kp but drops precipitously for Kp> 6.

[8] To construct an empirical model for the midnight, dawn, and postnoon sectors and separately for lower and upper band chorus, we first divide the data into 10% quantile bins in Kp and λ and compute the mean value of B_w^2 in this 10×10 grid. Next, we use linear regression to fit the logarithm of $< B_w^2 >$ to a polynomial of order up to 2 (including an interaction term) of the form:

$$log(< B_w^2 >) = w_0 + w_1 \text{Kp} + w_2 \lambda + w_3 \text{Kp}\lambda + w_4 \text{Kp}^2 + w_5 \lambda^2 \quad (1)$$

where the weights, w_n, are provided Table 1. We apply a stepwise fitting technique in which weights for the full model are first estimated, and terms are successively removed (as indicated by the weights being identically equal to zero in Table 1) if they do not contribute to the model in a statistically significant way. Specifically, a term is removed if the p-value is greater than 0.1 for an F test of the change in the sum of the squared error for a model with and without the term.

[9] In order to evaluate the goodness of fit of the regression models, we report the coefficient of determination, R^2, for each model in the last column of Table 1. R^2 varies from 0 to 1 and is interpreted as the percentage of variation in the bin-averaged data that can be explained by the model. The models perform better (higher values of R^2) in the midnight and dawn sectors and poorer in the postnoon sector. This is likely related to the relative data coverage in each sector. More samples available for averaging appears to result in smoother variation in the bin-averaged quantities, which in turn results in better fitting by the quadratic model. Conversely, the bin-averaged quantities in the postnoon sector are patchier. The model attempts to smooth this patchiness resulting in higher residual error and lower values of R^2. The meaning of R^2 and the relative values for different models can be better visualized with the figure included in the supporting information, which directly compares the bin-averaged quantities to the output of the model.

[10] Based on the output of dawn and postnoon models, we next construct an ad hoc model for the prenoon sector. For lower band chorus, we note that the functional dependence on both Kp and λ changes from quadratic in the dawn sector to linear in the postnoon sector. We do not believe that these changes result from issues involving data coverage but are indeed consistent with past work showing that chorus in the noon sector has a weaker dependence on geomagnetic activity and that the peak in wave power can occur at latitudes well above 15° [*Li et al.*, 2009; *Bunch et al.*, 2012].

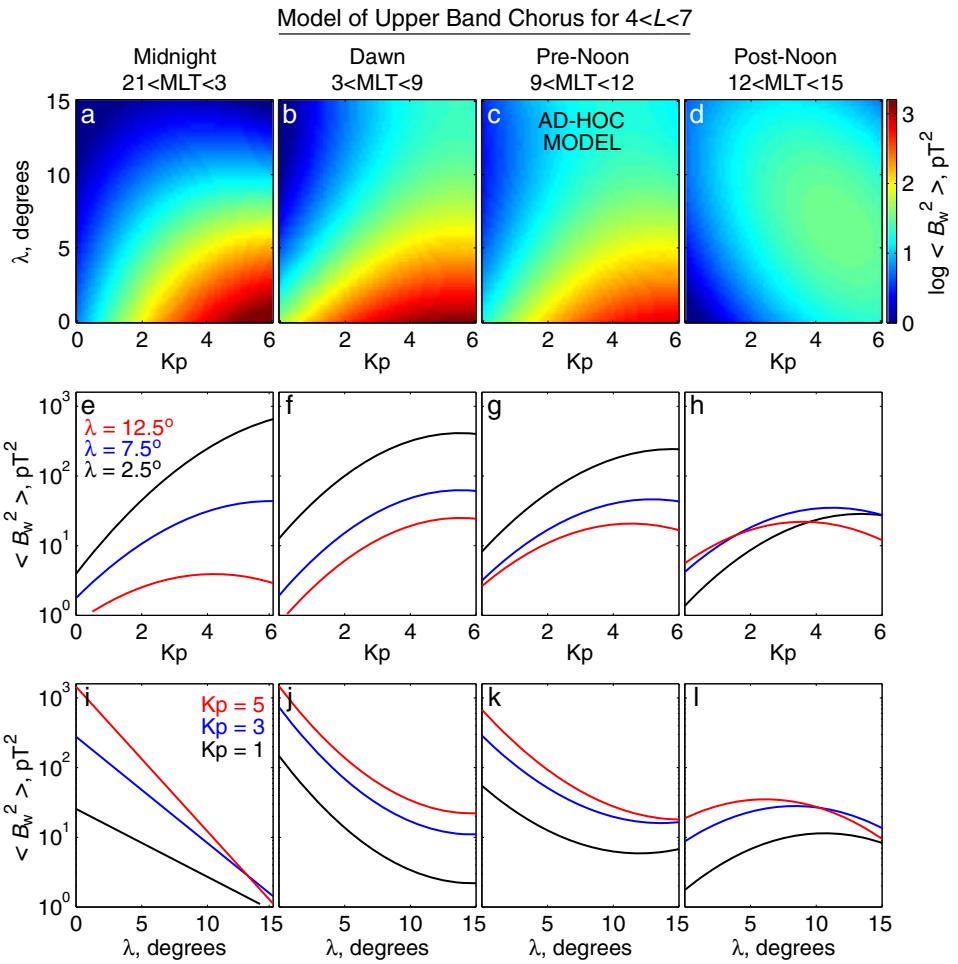

Figure 2. Two-dimensional output of the upper band chorus model for each of four local time sectors (a, b, c, d). Variation with Kp at three values of λ (e, f, g, h). Variation with λ for three values of Kp (i, j, k, l).

However, waves in the prenoon sector tend to be of higher average amplitude than in the postnoon sector [*Golden et al.*, 2012]. Therefore, to construct the ad hoc prenoon lower band model, we take the Kp and λ functional dependencies from the postnoon sector but scale B_w upward such that the maximum amplitudes are similar to those modeled in the dawn sector as shown in Figure 1g. For upper band chorus, there is less guidance in the literature on the global wave distribution (excluding, of course, analysis of CRRES data). To construct the ad hoc prenoon upper band model, we first note that wave amplitudes in the postnoon sector (Figure 2d) are significantly depressed compared with the dawn sector (Figure 2b). It may be that the lower energy source electrons that generate upper band chorus have poor access to the postnoon sector and are instead convected outward before reaching noon. Thus, for the ad hoc model, we have chosen to simply average the dawn and postnoon models to construct the prenoon model (Figure 2c). Since the prenoon models are constructed from scaled or averaged versions of models constructed in other local time sectors, the values of R^2 are $\sim$1 but are not statistically meaningful.

3. Discussion

[11] We have constructed quadratic fits to mean of B_w^2 for lower and upper band chorus as a function of Kp and λ for the midnight (21<MLT$\leq$3), dawn (3<MLT$\leq$9), and postnoon (12<MLT$\leq$15) sectors and presented an ad hoc model for the prenoon (9<MLT$\leq$12) sector. The empirical models are valid for 4$\leq$ L $\leq$7, $|\lambda| < 15°$ and Kp$\leq$ 6. Our results are generally consistent with previous studies, and our key contribution is the quantification of latitudinal and geomagnetic dependencies in a manner that is easily incorporated into quasi-linear diffusion models.

[12] The two-dimensional output of the models is shown in Figures 1 and 2, and for visual clarity, the bottom two rows show the variation with Kp for fixed values of λ and the variation of with λ for fixed values of Kp. For lower band chorus, we find that wave intensities generally increase with geomagnetic activity with waves in the dawn sector having the strongest Kp dependence (Figure 1j). Perhaps most striking are trends with λ, with waves in the midnight sector generally falling off with latitude, steady increases with latitude near noon, and waves at dawn peaking in the range of 5–10°. Further, in the midnight sector, the latitudinal dependence is different at different levels of geomagnetic activity (Figure 1m). For low activity levels, the latitudinal variation is relatively flat but the latitudinal falloff becomes increasingly steep for increasing Kp. In the dawn and noon sectors, the waves increase in amplitude with increasing Kp but the shape of the latitudinal variation remains relatively unchanged.

[13] Upper band chorus (Figure 2) is significantly weaker than lower band chorus but follows the trend of increasing amplitude with Kp. In the midnight and dawn sectors, wave amplitudes rapidly decrease off the equator. In the midnight sector, the latitudinal variation steepens with increasing Kp (Figure 2i) while at dawn the shape of the latitudinal dependence remains relatively constant (Figure 2j), similar to the effect seen in the lower band.

[14] The dual role of chorus in acceleration and loss of electrons necessitates accurate parametrization of the waves. For example, the latitudinal distribution of lower band chorus can significantly change the balance between acceleration and loss [e.g., *Shprits et al.*, 2006, Figure 4]. Relativistic electrons with near-loss cone pitch angles can be in first-order cyclotron resonance with chorus waves only at latitudes above $\sim 15^\circ$. Thus, if waves are confined to the geomagnetic equator, such as in the midnight sector, scattering losses will be reduced, but high-pitch angle electrons may still undergo efficient local acceleration. On the other hand, if waves are strong only at high latitude and weak at low latitude, such as in the noon sector, the net effect of wave scattering may be loss to the atmosphere, as dimensionless pitch angle scattering rates are usually larger than dimensionless energy scattering rates, and energy diffusion is not efficient for low-pitch angle particles that resonate with waves at high latitudes. Further, in the midnight sector, the fast decay of wave intensity with latitude during disturbed conditions favors acceleration whereas the relatively constant profiles at low activity may result in a net loss of electrons. Future studies will use the wave models presented here and may show differences in the net effect of chorus for different levels of geomagnetic activity.

[15] **Acknowledgments.** This work was supported by NASA award NNX09AF51G and NSF award 0902846.

[16] The Editor thanks two anonymous reviewers for assistance evaluating this paper.

References

Agapitov, O., V. Krasnoselskikh, Y. V. Khotyaintsev, and G. Rolland (2012), Correction to "A statistical study of the propagation characteristics of whistler waves observed by Cluster", *Geophys. Res. Lett.*, *39*, L24102, doi:10.1029/2012GL054320.

Anderson, R., D. Gurnett, and D. Odem (1992), CRRES plasma wave experiment, *J. Spacecraft Rockets*, *29*(4), 570.

Bunch, N. L., M. Spasojevic, and Y. Y. Shprits (2011), On the latitudinal extent of chorus emissions as observed by the Polar Plasma Wave Instrument, *J. Geophy. Res.*, *116*, A04204, doi:10.1029/2010JA016181.

Bunch, N. L., M. Spasojevic, and Y. Y. Shprits (2012), Off-equatorial chorus occurrence and wave amplitude distributions as observed by the Polar Plasma Wave Instrument, *J. Geophy. Res.*, *117*, A04205, doi:10.1029/2011JA017228.

Burtis, W. J., and R. A. Helliwell (1976), Magnetospheric chorus: Occurrence patterns and normalized frequency, *Planet. Spa. Sci.*, *24*, 1007, doi:10.1016/0032-0633(76)90119-7.

Golden, D. I., M. Spasojevic, W. Li, and Y. Nishimura (2012), An empirical model of magnetospheric chorus amplitude using solar wind and geomagnetic indices, *J. Geophy. Res.*, *117*, A12204, doi:10.1029/2012JA018210.

Haque, N., M. Spasojevic, O. Santolík, and U. S. Inan (2010), Wave normal angles of magnetospheric chorus emissions observed on the Polar spacecraft, *J. Geophy. Res.*, *115*, A00F07, doi:10.1029/2009JA014717.

Johnson, M., and J. Kierein (1992), Combined release and radiation effects satellite (CRRES): Spacecraft and mission, *J. Spacecraft Rockets*, *29*(4), 556.

Kim, K.-C., Y. Shprits, D. Subbotin, and B. Ni (2012), Relativistic radiation belt electron responses to GEM magnetic storms: Comparison of CRRES observations with 3-D VERB simulations, *J. Geophys. Res.*, *117*, 8221, doi:10.1029/2011JA017460.

Ledocq, M. J., D. A. Gurnett, and R. R. Anderson (1994), Electron number density fluctuations near the plasmapause observed by the CRRES Spacecraft, *J. Geophys. Res.*, *99*, 23,661, doi:10.1029/94JA02294.

Li, W., Y. Y. Shprits, and R. M. Thorne (2007), Dynamic evolution of energetic outer zone electrons due to wave-particle interactions during storms, *J. Geophys. Res.*, *112*(10), 220, doi:10.1029/2007JA012368.

Li, W., et al. (2009), Global distribution of whistler-mode chorus waves observed on the THEMIS spacecraft, *Geophys. Res. Lett.*, *36*, L09104, doi:10.1029/2009GL037595.

Meredith, N. P., R. B. Horne, R. M. Thorne, and R. R. Anderson (2003a), Favored regions for chorus-driven electron acceleration to relativistic energies in the Earth's outer radiation belt, *Geophys. Res. Lett.*, *30*(16), 1871, doi:10.1029/2003GL017698.

Meredith, N. P., M. Cain, R. B. Horne, R. M. Thorne, D. Summers, and R. R. Anderson (2003b), Evidence for chorus-driven electron acceleration to relativistic energies from a survey of geomagnetically disturbed periods, *J. Geophys. Res.*, *108*(A6), 1248, doi:10.1029/2002JA009764.

Meredith, N. P., R. B. Horne, A. Sicard-Piet, D. Boscher, K. H. Yearby, W. Li, and R. M. Thorne (2012), Global model of lower band and upper band chorus from multiple satellite observations, *J. Geophy. Res.*, *117*, A10225, doi:10.1029/2012JA017978.

Millan, R. M., and D. N. Baker (2012), Acceleration of particles to high energies in Earth's radiation belts, *Space Sci Rev*, *173*, 103, doi:10.1007/s11214-012-9941-x.

Moldwin, M. B., L. Downward, H. K. Rassoul, R. Amin, and R. R. Anderson (2002), A new model of the location of the plasmapause: CRRES results, *J. Geophys. Res.*, *107*(A11), 1339, doi:10.1029/2001JA009211.

Shprits, Y. Y., R. M. Thorne, R. B. Horne, S. A. Glauert, M. Cartwright, C. T. Russell, D. N. Baker, and S. G. Kanekal (2006), Acceleration mechanism responsible for the formation of the new radiation belt during the 2003 Halloween solar storm, *Geophys. Res. Lett.*, *33*, L05104, doi:10.1029/2005GL024256.

Shprits, Y. Y., N. P. Meredith, and R. M. Thorne (2007), Parameterization of radiation belt electron loss timescales due to interactions with chorus waves, *Geophys. Res. Lett.*, *34*, L11110, doi:10.1029/2006GL029050.

Shprits, Y. Y., S. R. Elkington, N. P. Meredith, and D. A. Subbotin (2008a), Review of modeling of losses and sources of relativistic electrons in the outer radiation belt I: Radial transport, *J. Atmos. Solar-Terr. Phys.*, *70*, 1679, doi:10.1016/j.jastp.2008.06.008.

Shprits, Y. Y., D. A. Subbotin, N. P. Meredith, and S. R. Elkington (2008b), Review of modeling of losses and sources of relativistic electrons in the outer radiation belt II: Local acceleration and loss, *J. Atmos. Solar-Terr. Phys.*, *70*, 1694, doi:10.1016/j.jastp.2008.06.014.

Subbotin, D. A., Y. Y. Shprits, and B. Ni (2011), Long-term radiation belt simulation with the VERB 3-D code: Comparison with CRRES observations, *J. Geophy. Res.*, *116*, A12210, doi:10.1029/2011JA017019.

Thorne, R. M. (2010), Radiation belt dynamics: The importance of wave-particle interactions, *Geophys. Res. Lett.*, *37*, L22107, doi:10.1029/2010GL044990.